Infrasound propagation in realistic atmosphere using nonlinear ray theory

Olaf Gainville, Philippe Blanc Benon

10ème **C**ongrès **F**rançais d'**A**coustique

Lyon, 12-16 Avril 2010

Infrasound propagation in realistic atmosphere using nonlinear ray theory

Olaf Gainville[1], Philippe Blanc-Benon[2]

[1] CEA/DAM/DIF, Arpajon, F-91287, France, olaf.gainville@cea.fr

[2] CNRS, LMFA UMR 5509, Ecole centrale de lyon, 36 Av. Guy de Collongue, 69134 Ecully Cedex, France, philippe.blanc-benon@ec-lyon.fr

Using ray theory, long range propagation of infrasound through the atmosphere is modeled in the framework of the Comprehensive Nuclear-Test-Ban Treaty. In atmospheric propagation, the high frequency hypothesis is based on the assumption that space and time scales of atmospheric properties (temperature, wind, density) are much larger than acoustic wave scales. An operational 3D nonlinear ray tracing code is developed to compute the temporal pressure signature at receivers. The global pressure signature at the receiver is the sum of eigenray contributions that link the source to the receiver. They are obtained by solving a generalized Burgers' equation along each eigenray taking into account nonlinear effects, shear and bulk viscosity absorption and molecular vibrational relaxation mechanisms. This equation is solved using a Fourier Galerkin spectral scheme. Specific developments are performed to pass through caustics and take into account ground reflection. The propagation of infrasound emitted by a motionless point source in a realistic atmosphere will illustrate the analysis. To quantify the validity limits of our approach, we investigate effects of the wind, atmospheric absorption, nonlinearities, refraction and scattering by small atmospheric scales on observed phase kinds, their travel time and their waveform. To estimate the nonlinearity effects relative to the linear dissipative effects we evaluate the Gol'dberg number. We note that nonlinear mechanisms are important to model the evolution of infrasonic waveform signatures. The 'N' and the 'U' measured waveform shape of, respectively, thermospheric and stratospheric paths are associated with nonlinear mechanisms. Nonlinearities are weak but the development of nonlinear models is necessary in order to characterize the source yield. Comparisons will be made with results available in the literature and recent numerical simulations based on Navier-Stokes equations.

1 Introduction

A strong motivation for continuing infrasonic research is for understanding atmospheric acoustics in the context of the Comprehensive Nuclear-Test-Ban Treaty. The International Monitoring System develops a sixty barometric stations network which should be able to detect one kiloton yield explosion anywhere on the globe. Explosion studies are necessary to evaluate the detection capability of this network and to develop tools for infrasound record analysis. In this context, the Commissariat à l'Energie Atomique, in collaboration with the Laboratoire de Mécanique des Fluides et d'Acoustique, has developed a capability for discrimination and characterization of large explosive sources.

In this article, we investigate the long range propagation of infrasound in the conditions of a High Explosive experiment named Misty Picture [11]. We study links between the source yield and microbarometric station pressure signatures. First we present the Misty Picture experiment, its modelisation and the ray tracing method used to model the evolution of nonlinear pressure signatures along rays. Second, we quantify influence of nonlinear effects. Last, we perform comparaison between simulation, empirical law and measurements of infrasound signature maximum overpressure and energy.

2 Misty Picture experiment

Misty Picture was a high explosive test sponsored by the US Defense Nuclear Agency. It was detonated at 10 :00 MDT (16 :00 UT) on the 14^{th} May 1987 at White Sands Missile Range in New Mexico (US). The explosive charge consisted of 4685 tons of ANFO (Ammonium Nitrate and Fuel Oil) arranged into a 27-meters diameter fiberglass hemispheric container installed on the ground. The resulting airblast provided the scaled equivalent airblast of an 8 kT nuclear device. The primary objective of the test was to provide an airblast, dust cloud and ground shock environment for the US Department of Defense [11].

Three laboratories recorded infrasound emitted by this explosive test at distances from 7 km to 1200 km as presented in Figure 1 : the Sandia National Laboratory [15], the Los Alamos National Laboratory [19] and the French Commissariat à l'Energie Atomique [1, 5, 6]. The event was instrumented with 23 barometric stations. Because of background wind noise, only 21 of the 23 pressure signatures allow an observation of arrivals. Six stations between the source and 100 km detected a tropospheric arrival. Five stations between 100 km and 220 km detected both stratospheric and tropospheric arrivals whereas the four stations between 220 km and 450 km detected thermospheric arrivals. The six farthest stations, between 700 km and 1,200 km towards West, detected multiple stratospheric arrivals only.

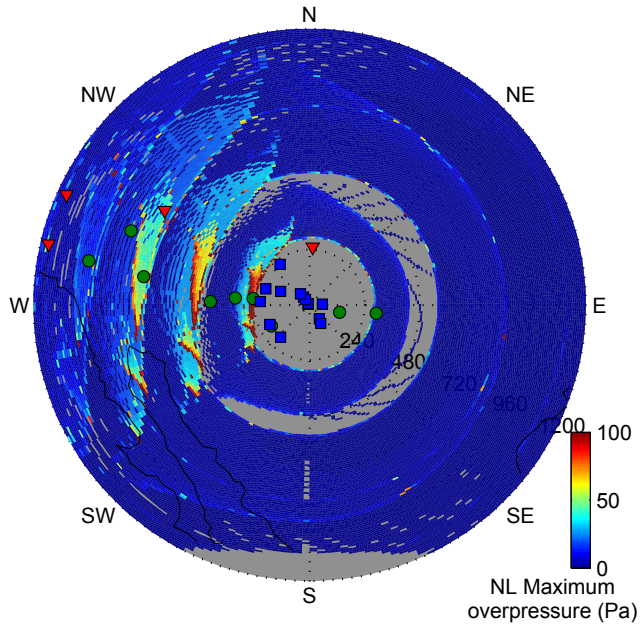

FIG. 1: Maximum overpressure map of stratospheric and thermospheric phases simulated with nonlinear ray tracing method. Infrasonic measurements perform by (▼) Los Alamos National Laboratory [19], (■) Sandia National Laboratory [15] and (●) Commissariat à l'Energie Atomique [1].

3 Infrasound modeling

In this section, we describe the source, the atmosphere and the nonlinear ray tracing model used to model the long range propagation of infrasound generated by the Misty Picture event.

3.1 Explosion modeling

The Misty Picture explosion yield is equivalent to 3840 tons of trinitrotoluene (TNT) [10, 15]. The shock wave pressure signature close to the source is described by the maximum overpressure, the positive phase duration and the waveform which are estimated using the Kinney & Graham empirical models [9, 5]. 4,000 m away from Misty Picture ground zero, maximum overpressure is 3040 Pa and time duration is $t_d = 0.67$ s. Main frequency is around 0.3 Hz. This signature is used as initial condition in infrasound models as presented in details by Gainville [5, 6].

3.2 Atmospheric model

To model the long range propagation of infrasound, we use an inhomogeneous stratified atmosphere which is a combination of measurements [15] with empirical models [8]. Temperature and winds profiles are given for altitudes between the ground and 19 km by the rawinsonde launch from Stallion station and between 29 km and 73 km by the rocketsonde launch from White Sand Missile Range. These measurements are completed by statistical temperature MSIS-90 and wind HMW-93 profiles up 73 km. Composition profiles, thermodynamic relations and atmospheric sound absorption coefficients of Sutherland & Bass [17] are also used. Absorption and wave dispersion take into account shear viscosity, bulk viscosity and molecular vibrational relaxation. See Gainville [5, 6] for a detailed presentation of atmospheric profiles.

3.3 Nonlinear ray tracing method

The ray tracing method models the propagation of acoustic waves in the geometrical acoustics limits. Geometrical acoustics is the study of acoustic wave fronts propagating in the high frequency hypothesis. In atmospheric propagation, the high frequency hypothesis assumes that space and time scales of atmospheric properties (temperature, wind, density) are much larger than acoustic wave scales. For a detailed presentation of the geometrical acoustic theory, we refer the reader to Candel [2]. For a detailed presentation of the ray tracing code and its validation, we refer the reader to Gainville & al. [7, 5, 6]. Our ray tracing code solves ray tracing equations and geodesic elements equations to compute ray trajectory and amplitude variations using wave action conservation law. We use an efficient shooting method to determine all the eigenrays that link the source to the station. Each eigenray is associated with an arrival at the station. The group velocity of the ray at the station provides the trace velocity and the azimuth of the wave. The global pressure signature at the receiver is the sum of eigenray pressure signature contributions. These pressure signatures are obtained by solving a generalized Burgers' equation along each eigenray. This generalized Burgers' equation takes into account nonlinear effects, shear and bulk viscosity absorption and molecular vibrational relaxation mechanisms. The pressure signature p' is normalised using the wave action conservation law as :

$$u(\xi,t) = \left(\frac{\nu}{k\rho_0 c_0^3}\right)^{1/2} p'\left(\vec{x}(t) + \xi\vec{n}/k, t\right), \qquad (1)$$

where ξ is a scaled distance, t is the time curvilinear abscissa along the ray and ν is the convected volume [5] which is proportionnal to the classical ray tube section [14]. $\vec{x}(t)$ is the trajectory of the wave front and $\vec{k} = k\vec{n}$ the local wave vector. c_0 is the sound speed and ρ_0 is the density. The extended Burgers' equation is solved using a Fourier Galerkin spectral scheme :

$$\frac{\partial\tilde{u}(q,t)}{\partial t} = -\Gamma(kq,t)\tilde{u} - \imath\beta\left(\frac{c_0 k}{\rho_0\nu}\right)^{1/2}\frac{kq}{2}\widetilde{(u^2)}, \qquad (2)$$

where kq is the acoustic wavelength. The dissipative and dispersive part of $\Gamma(kq,t)$ models thermoviscous and molecular relaxation mechanisms [17, 5]. The coefficient $\beta = \frac{1+\gamma}{2}$ is the nonlinear coefficient. Variables depend on the underlying atmospheric state at the position $x(t)$. This differential equation system is integrated along rays from the source to the receiver. Specific developments are performed to pass through caustics and take into account ground reflection. This method is particularly efficient in modeling the propagation of infrasound, particularly in three dimensions. But it is limited in the case of low frequency sources, such as the Misty Picture event, because the model does not incorporate wave diffraction.

4 Nonlinearity and atmospheric absorption effects

Nonlinear and atmospheric absorption effects are investigated on the pressure signature evolution along ray paths for the Misty Picture event. The shock formation time t_{shock} quantifies nonlinearity effects relative to the propagation distance. The Gol'dberg number G [16] quantifies nonlinearity effects relative to linear dissipative effects for a given pressure signature. These numbers are defined from the Burgers' equation as :

$$t_{\text{shock}} = \frac{\rho_0 c_0^2}{\beta f_{\text{w}} p_{\text{w}}}, \quad \text{and,} \quad G = \frac{\beta p_{\text{w}}}{\delta \rho_0 f_{\text{w}}},$$

where β is the nonlinear coefficient, $\delta = |\Gamma|/kq$ is the absorption coefficient [14], p_{w} is the wave amplitude and f_{w} is the wave central frequency. These two numbers are evaluated for the Misty Picture event along eigenrays which arrived at Alpine, White River and Roosevelt stations. Pressure signatures computed along these rays by solving the generalized Burgers' equation are used to evaluate the central frequency f_{w} and amplitude p_{w}. The shock formation time and the Gol'dberg number are plotted in Figure 2.

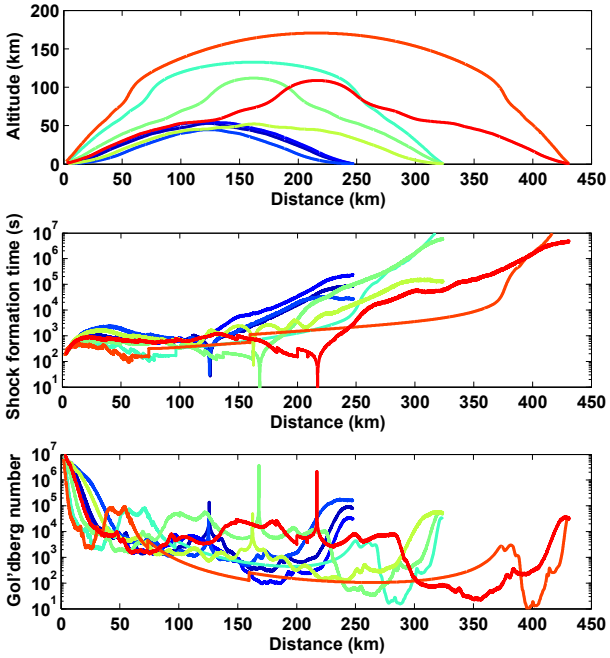

FIG. 2: Nonlinear effects for the Misty Picture event. From top to bottom, ray paths, the shock formation time and the Gol'dberg number are plotted for Alpine (248 km), White River (324 km) and Roosevelt (431 km) station eigenrays.

Shock formation time mainly increases during the propagation whereas the Gol'dberg number decreases. This is associated to the increase of the pressure signature duration and the decrease of its amplitude. The shock formation time evolves quickly close to the source from 0 s to 100 s and after 10 km of propagation it remains between 100 and 1000 s except near caustics where it decreases to 0 because of caustic signature amplitude singularity. The Gol'dberg number evolves symmetrically with a singularity near caustics and the source.

As presented on Figure 2, the shock formation time is of the order of 100 s, *i.e.* a distance of 30 km. With only nonlinear mechanisms, after a propagation time of 100 s, the pressure signature evolves as a 'N' wave, independently of the waveform source shape. Nonlinearities are weak and it is a cumulative process efficient at long range. The propagation time to the barometric station (∼1000 s) is 10 times the shock formation time. Then, pressure signatures at the station, in absence of competitive processes, are close to an 'N' wave.

For the Misty Picture experiment, the Gol'dberg number is greater than approximatively 17 (cf. Figure 2), which means that non linearities are dominant relatively to linear absorption mechanisms. This Gol'dberg number limit is obtained by Rogers & Gardner [16] by equalizing nonlinear absorption with linear viscosity and molecular relaxation absorption mechanisms. This number can be found numerically by a parametric study of the Burgers' equation. The pressure signature at receiver is mainly dependent on nonlinearities, but absorption mechanisms are important to study the shock rise time or for lower amplitude sources. When, in an application, the Gol'dberg number is *a priori* unknown, the full generalized Burgers' equation should be solved.

5 Waveform signature analysis

Phase identification at barometric station located between 200 km and 400 km in the West direction of the source allows us to find two stratospheric paths Is_I and Is_{II} and a thermospheric path It_a at White River (Figure 3). However, the ray tracing method predicts only one stratospheric path and one thermospheric path at White River. Pressure signatures measured and computed using linear ray tracing, nonlinear ray tracing and parabolic equation [3] for the White River station are plotted in Figure 3. Comparisons to finites differences method are also performed in Marsden & al. [12].

Arrival times are globally in agreement between measurements, ray tracing and parabolic equation methods except for modeled thermospheric paths which arrived approximatively 50 s before measurements. This difference is due to the atmospheric models which should under estimate effective celerity in the high atmosphere. Signature amplitudes are globally in good agreement except near caustics where the amplitude is overestimated with the ray tracing method. This is the case of the first stratospheric path. Ray tracing simulations over estimate the amplitude whereas the parabolic equation method amplitude is realistic. Linear simulations over estimate the amplitude of the thermospheric arrival whereas nonlinear ray tracing agrees with the measurements. The nonlinear computation of the waveform allows the reconstitution of a 'U' pressure signature for the stratospheric path and of a 'N' pressure signature thermospheric path.

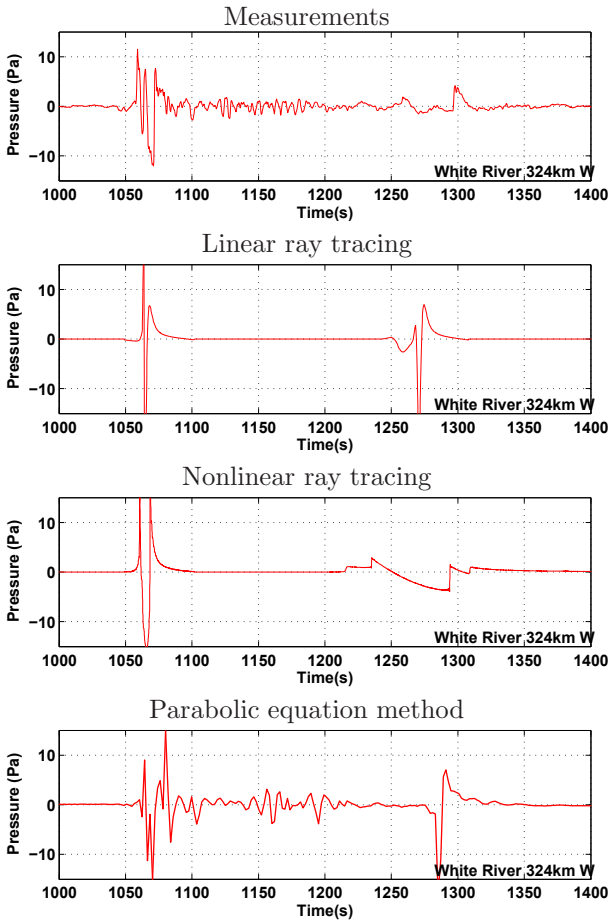

FIG. 3: Pressure signatures at White River station (324 km).

6 Maximum overpressure and energy signature analysis

To estimate the source energy from infrasonic measurements, empirical laws which link source yield W to the maximum overpressure are often used [4]. These empirical laws are based on a cylindrical scaling law $R/W^{1/2}$, with R the distance to the source. Whitaker & al. have calibrated such law using explosion experiments [13, 18]. This law take into acount of the mean wind in the stratosphere and are defined for stratospheric paths.

Comparison between measured, Whitaker's empirical law, linear ray tracing, non linear ray tracing and parabolic equation maximum overpressure is presented in Figure (4). Computations are performed in the West direction for the Misty Picture configuration. Measured maximum overpressure of each arrival of each station in the West direction are plotted with direct arrivals in blue, stratospheric arrivals in green and thermospheric arrivals in red. For ray tracing methods, each arrival is visible and caustics appear as peaks of the maximum overpressure. For the parabolic method, only the maximum overpressure of the full signal at the station is computed.

In the first shadow zone, *i.e.* between 30 and 80 km/kt$^{1/2}$ in Figure (4), the empirical law over estimates the maximum overpressure whereas the parabolic equation method is more in agreement with measurements. For stratospheric arrivals, empirical law, parabolic equation method and nonlinear ray tracing results are in agreement with measurements (green points) between 80 and 130. For stratospheric arrival observed at the station at 150 and for thermospheric arrivals (red points), only the nonlinear ray tracing method agrees with measurements. In addition, linear ray tracing and linear parabolic method are not in agreement for all arrivals. This allows us to conclude that the maximum overpressure is quite dependant on the signal sampling both for measurements and for simulations. However, this signature caracteristic is more usefull to evaluate the source yield than a direct comparison of pressure signature as performed in the section 5. The map of the maximum overpressure for stratospheric and thermospheric phases is also presented in figure (1). This illustrate wind effets on the maximum overpressure.

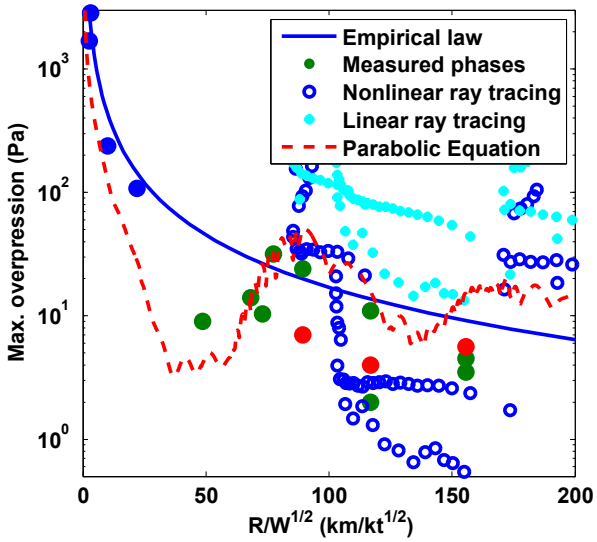

FIG. 4: Maximum overpressure as a fonction of the horizontal propagation distance.

In addition to the maximum overpressure, the energies of arrivals are computed for measurements and code simulations and presented in Figure 5. This energy is evaluated in the 0.05 to 0.5 frequency bandwidth in which parabolic results are available. First we observed a very good agreement between linear ray tracing and linear parabolic method results. For stratospheric and thermospheric arrivals linear simulations overestimate measurements whereas nonlinear simulation is quite more in agreement.

It appears from simulations that the frequency band energy is a more robust signature caracteristic than the maximum overpressure. This last one is too sensitive to signal sampling and to sensor pass-band.

7 Conclusion

We observe that both nonlinearity and scattering have influence on infrasonic pressure signature at stations. Nonlinearities allow to find the 'N' and the 'U' waveforms measured for respectively thermospheric and stratospheric paths. Nonlinearity is a weak mechanism which dominates linear absorption effects during the propagation, for an event of the Misty Picture energy class. Scattering influences both the overpressure signature waveform and energy, especially for the stratos-

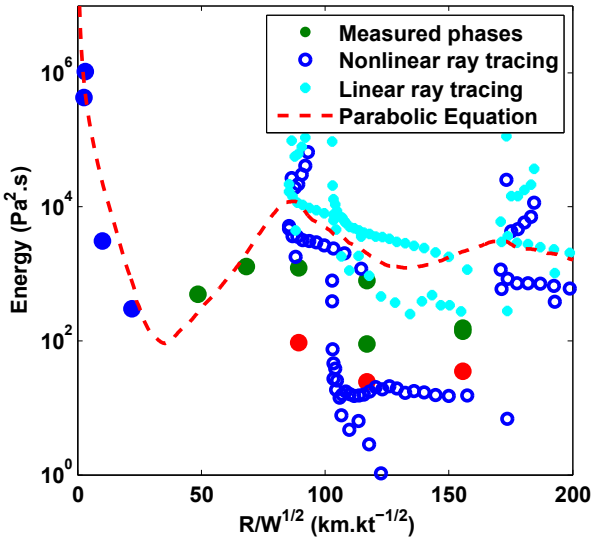

FIG. 5: Phase energy in the frequency range 0.05 to 0.5 Hz as a fonction of the propagation distance.

pheric paths. We also observed that the energy in a frequency band seems a robust signature caracteristic to evaluate the source yield from infrasound measurements. In spite of these results, comparisons between simulations and measurements remain difficult because meteorological conditions remain uncertain.

Références

[1] BLANC, E. Mesures ionosphériques et microbarographiques – Expérience Misty Picture. Tech. Rep. 370/88, CEA, Sep. 1988.

[2] CANDEL, S. M. Numerical solution of conservation equations arising in linear wave theory : Application to aeroacoustics. *J. Fluid Mech. 83*, 3 (1977), 465–493.

[3] DALLOIS, L. *Propagation des ondes acoustiques dans les milieux en mouvement : extension grand angle de l'approximation parabolique*. PhD thesis, École Centrale de Lyon, Lyon, 2000.

[4] EVERS, L., AND HAAK, H. Seismo-acoustic analysis of explosions and evidence for infrasonic forerunners. In *Infrasound Technology Workshop* (Fairbanks, Sep. 2006), University of Alaska.

[5] GAINVILLE, O. *Modélisation de la propagation atmosphérique des ondes infrasonores par une méthode de tracé de rayons non linéaires*. PhD thesis, École centrale de Lyon, mai 2008. Num. 2008-07.

[6] GAINVILLE, O., BLANC-BENON, P., BLANC, E., ROCHE, R., MILLET, C., PIVER, F. L., DESPRES, B., AND PISERCHIA, P. F. *Misty Picture : A Unique Experiment for the Interpretation of the Infrasound Propagation from Large Explosive Sources*. Springer, 2009, pp. 575–598.

[7] GAINVILLE, O., BLANC-BENON, P., PISERCHIA, P. F., AND SCOTT, J. Infrasound propagation in realistic atmosphere : numerical modelling using ray theory and comparison with experiments. In *12th Long Range Sound Propagation Symposium* (New Orleans, USA, 25-26 oct. 2006).

[8] HEDIN, A. E., FLEMING, E. L., MANSON, A. H., SCHMIDLIN, F. J., AVERY, S. K., CLARK, R. R., FRANKE, S. J., FRASERA, G. J., TSUDA, T., VIAL, F., AND VINCENT, R. A. Empirical wind model for the upper, middle and lower atmosphere. *J. Atmos. Terr. Phys. 58* (1996), 1421–1447.

[9] KINNEY, G. F., AND GRAHAM, K. J. *Explosive shocks in air*, berlin heidelberg ed. Springer Verlag, New York, Tokyo, 1985.

[10] KOPER, K. D., WALLACE, T. C., REINKE, R. E., AND LEVERETTE, J. A. Empirical scaling laws for truck bomb explosions based on seismic and acoustic data. *Seismological Society of America 92*, 2 (March 2002), 527–542.

[11] LEHR, L. D. Misty Picture event - test execution report. Tech. Rep. ADA283521, Defence nuclear agency, Washington, Nov. 1987.

[12] MARSDEN, O., VAYNO, L., BOGEY, C., AND BAILLY, C. Study of long-range infrasound propagation with high-performance numerical schemes applied to the euler equations. In *13th Long Range Sound Propagation Symposium* (Lyon, France, 16-17 oct. 2008), pp. 201–216.

[13] MUTSCHLECNER, J. P., WHITAKER, R. W., AND AUER, L. H. An empirical study of infrasonic propagation. Tech. rep., Los Alamos National Lab., Los Alamos, NM (US), 1999.

[14] PIERCE, A. D. *Acoustics : An Introduction to Its Physical Principles and Applications*. Acoustical Society of America, 1994.

[15] REED, J. W., CHURCH, H. W., AND HUCK, T. W. Misty Picture weather-watch and microbarograph project : experiments 9412-14-18. Sand–87-2978c, Sandia National Laboratories, 1987.

[16] ROGERS, P. H., AND GARDNER, J. H. Propagation of sonic booms in the thermosphere. *J. Acoust. Soc. Am. 67*, 1 (1980), 78–91.

[17] SUTHERLAND, L. C., AND BASS, H. E. Atmospheric absorption in the atmosphere up to 160km. *J. Acoust. Soc. Am. 115 (3)*, 115 (3) (March 2004), 1012–1032.

[18] WHITAKER, R., SONDOVAL, T., AND MUTSCHLECNER, J. Recent infrasound analysis. In *25th Seismic Res. Rev.* (Tucson, Arizona, Sep. 2003).

[19] WHITAKER, R. W., MUTSCHLECNER, J. P., DAVIDSON, M. B., AND NOEL, S. D. Infrasonic observations of large-scale HE events. In *4th Long Range Sound Propagation Symposium* (Virginia, USA, 16-17 May 1990), pp. 133–141.